Received: 28 April 2020 | Revised: 13 August 2020 | Accepted: 25 August 2020

DOI: 10.1002/aoc.6005

Check for updates

Applied Organometallic Chemistry WILEY

FULL PAPER

One-pot multicomponent synthesis of novel 2-(piperazin-1-yl) quinoxaline and benzimidazole derivatives, using a novel sulfamic acid functionalized Fe_3O_4 MNPs as highly effective nanocatalyst

Zohreh Esam[1] | **Malihe Akhavan**[1,2] | **Ahmadreza Bekhradnia**[3,4]

[1]Student Research Committee, Department of Medicinal Chemistry, Faculty of Pharmacy, Mazandaran University of Medical Sciences, Sari, Iran

[2]Department of Medicinal Chemistry, Faculty of Pharmacy, Ayatollah Amoli Branch, Islamic Azad University, Amol, Iran

[3]Department of Medicinal Chemistry, Mazandaran University of Medical Sciences, Sari, Iran

[4]Department of Chemistry And Biochemistry, 103CBB, Montana State University, Bozeman, Montana, USA

Correspondence
Ahmadreza Bekhradnia, Department of Medicinal Chemistry, Mazandaran University of Medical Sciences, Sari, Iran.
Email: a.bekhradnia@gmail.com; ahmadreza.bekhradnia@montana.edu

Funding information
Faculty of Pharmacy, Mazandaran University of Medical Sciences

The immobilization of sulfonic acid on the surface of Fe_3O_4 magnetic nanoparticles (MNPs) as a novel acid nanocatalyst has been successfully reported. The morphological features, thermal stability, magnetic properties, and other physicochemical properties of the prepared superparamagnetic core–shell (Fe_3O_4@PFBA–Metformin@SO_3H) were thoroughly characterized using Fourier transform infrared (FTIR), X-ray diffraction (XRD), energy-dispersive X-ray spectroscopy (EDS), field-emission scanning electron microscopy (FESEM), transmission electron microscopy (TEM), thermogravimetric analysis–differential thermal analysis (TGA-DTA), atomic force microscopy (AFM), dynamic light scattering (DLS), Brunauer–Emmett–Teller (BET), and vibrating sample magnetometer (VSM) techniques. It was applied as an efficient and reusable catalyst for the synthesis of 2-(piperazin-1-yl) quinoxaline and benzimidazole derivatives via a one-pot multiple-component cascade reaction under green conditions. The results displayed the excellent catalytic activity of Fe_3O_4@PFBA–metformin@SO_3H as an organic–inorganic hybrid nanocatalyst in condensation and multicomponent Mannich-type reactions. The easy separation, simple workup, excellent stability, and reusability of the nanocatalyst and quantitative yields of products and short reaction time are some outstanding advantages of this protocol.

KEYWORDS
benzimidazole, nanocatalyst, N-Mannich base, quinoxaline, sulfamic acid

1 | INTRODUCTION

N-heterocyclic compounds are some of the most versatile building blocks in medicinal chemistry that are utilized in the most active bioorganic compounds.[1,2] Among these, quinoxaline (benzopyrazine) derivatives, especially 2-amino quinoxalines as well as benzimidazole moiety, play a vital role in the development of biological compounds with valuable activities, including antiviral, antibacterial, antimicrobial, antifungal, antimalarial, antidepressant, antidiabetic and kinase (c-Met) inhibitory, and anticancer effects.[3–5]

In addition, quinoxaline as a bioisostere of different heterocyclic systems such as benzimidazole, pteridine, quinazoline, quinoline, benzothiophene, pyridine, and pyrazine has become a significant portion of various bioactive small molecules in the pharmaceutical field.[6]

 © 2020 John Wiley & Sons, Ltd.

Because of the extensive activity of these scaffolds, the synthesis of the heterocyclic compounds as biologically active agents have always been at the center of attention. Although most of the reported protocols have their advantages, many of them suffer from disadvantages, that is, long reaction time, the use of toxic and/or expensive reagents, difficulty in separation of the catalyst from the reaction mixture, and recycling.[7–9]

Therefore, the development of sustainable and green protocols and efficient and recycling catalysts for the synthesis of quinoxaline and benzimidazole motifs is an important challenge associated with these protocols.

From this point of view, heterogenization of the homogeneous catalysts on appropriate supports rendered a great strategy for the design and preparation of superior heterogeneous organic–inorganic hybrid catalysts that not only exhibit better activity, stability, and selectivity but also permit facile catalyst recovery, which is one of the overarching principles of green chemistry.[10,11]

Among the myriad of solid carriers, Fe_3O_4 magnetic nanoparticles (MNPs) are attractive for the heterogenization of homogeneous catalysts because of their nano-size, nontoxic nature, easy preparation and functionalization procedures, and facile removal with the aid of a simple external magnet from the ultimate reaction mixture since their paramagnetic property.[12–15]

The surface of bare MNPs may be improved to form a protective shell. The shell can avoid aggregation and decline of the magnetic cores and make the support amenable for various chemical modifications to accommodate a variety of organic–inorganic nanocatalysts.

According to the literature, heteropolyanion-based ionic liquids,[16] manganese ferrite ($MnFe_2O_4$) nanopowder,[17] heterogeneous nano-U-Fe_2O_3-SO_3H,[18] nanostructured pyrophosphates $Na_2PdP_2O_7$,[19] sulfonated rice husk ash (RHA-SO_3H),[20] biopolymer-supported ferrite nanocatalysts,[21] and SO_3H-functionalized Zeolite-Y[22] were prepared and used as solid catalysts for the synthesis of benzimidazole and quinoxaline derivatives. Surface sulfonation of Fe_3O_4 MNPs by chlorosulfonic acid (HSO_3Cl) is also an appropriate, acceptable, quick, easy, and effective way to produce acidic heterogeneous nanocatalyst with high catalytic efficiency[23,24] in the synthesis of heterocyclic systems, specially benzimidazole and quinoxaline derivatives, which deserves more attention.

What adds to the importance of our research is the green synthesis of Mannich base derivatives of benzimidazole and quinoxaline using these nanocatalytic processes, which, despite being very important, has been abandoned in research.

Herein, the first step of this research was describing a green synthesis route for preparing of a leak-free and highly efficient multifunctional heterogeneous magnetic nanocatalyst via grafting sulfonic groups onto the surface of Fe_3O_4 MNPs coated with a novel Schiff-base layer consisting of metformin and p-formylbenzoic acid (PFBA) as an efficacious bridge. The latter portion has two functional heads: its COOH moiety, which has a strong affinity to Fe_3O_4 surface hydroxyl groups, and NH groups for the grafting of multi-SO_3H functionalities. Then, we investigated the utility of the newly synthesized organic–inorganic hybrid (Fe_3O_4@PFBA–metformin@SO_3H) as a core–shell-structured nanocatalyst for the synthesis of novel quinoxaline and benzimidazole derivatives via a multicomponent one-pot cascade reaction. The results of this research displayed the excellent catalytic activity of Fe_3O_4@PFBA–metformin@SO_3H in a multicomponent Mannich-type reaction. The Mannich reaction is a valuable organic reaction for the synthesis of various nitrogen-containing pharmaceuticals.[25] The chemical structure of our final N-Mannich base products consists of three important functional and bioactive parts: the core of 2-piperazinylquinoxaline or 2-piperazin-1-ylmethyl-1*H*-benzoimidazole, (substituted) isatin, and the amine-containing tail portion (semicarbazone, thiosemicarbazone, and metformin).

2 | EXPERIMENTAL SECTION

2.1 | Materials and methods

2.1.1 | General

All starting materials and chemicals used in this research were bought from Merck and Sigma-Aldrich chemical companies without further purification. All recorded melting points (m.p.) were taken in an open capillary tube on a Stuart scientific melting point apparatus and are uncorrected. Elemental analysis was performed on a Perkin–Elmer 2400 C, H, N analyzer, and values were within the acceptable limits of the calculated values. Fourier transform infrared (FTIR) spectra of all samples in our study were recorded in the subregion 400–4,000 cm^{-1} on Perkin–Elmer spectrum one instruments using potassium bromide discs. Mass spectra were obtained on an HP 5975 mass selective detector at 70 eV. The proton magnetic resonance ^1H and ^{13}C spectra were performed on Bruker 400 or 600 spectrometers using $CDCl_3$ and/or DMSO-d_6 as the solvent, all with tetramethylsilane (TMS) as the internal standard. The chemical shifts were reported in δ value as parts per million (ppm), and coupling constants (J) are expressed in hertz (Hz). The following abbreviations were used to explain the multiplicities: br, broad; s, singlet; d, doublet; and m,

multiplet. Spectral data (infrared [IR], mass, and nuclear magnetic resonance [NMR] spectra) confirmed the structures of the synthesized compounds. The progress and success of each step, as well as the purity determinations of the obtained compounds, were controlled and confirmed by thin-layer chromatography (TLC) on ready-made silica gel plates (Merck) using chloroform:methanol (9:1) as mobile phase. Spots were detected and visualized under UV light.

The X-ray diffraction (XRD) pattern related to the structural phases of the prepared catalyst was accomplished using a Jeol JEM-1010 electron microscope and JEOL JSM-6100 microscope with Cu kα radiation $\lambda = 1.54$ Å in the region of $2\Theta = 20°–80°$.

Atomic force microscopy (AFM) was utilized to determine the surface roughness of Fe_3O_4@PFBA–metformin@SO_3H MNPs using JPK-AFM (JPK Instruments AG, Berlin, Germany). The surface morphology and diameter of the catalyst nanoparticles (Fe_3O_4@PFBA–metformin@SO_3H) were studied by transmission electron microscopy (TEM) and scanning electron microscopy (SEM). TEM imaging of the nanocatalyst was performed using Philips EM028 TEM, Aachen, Germany. Energy-dispersive X-ray spectroscopy (EDX or EDS) analyses were performed. The elemental mapping and compositional analysis were performed by a Kevex, Delta Class I, equipped with the SEM instrument.

To characterize the magnetic property of modified and unmodified nanoparticles, a varying magnetic field from −10,000 to 10,000 on a BHV-S5 vibrating sample magnetometer (VSM) was utilized at room temperature (MDKFD, University of Kashan, Kashan, Iran). The particle size distribution and zeta potential of the Fe_3O_4@PFBA-metformin@SO_3H were determined by dynamic light scattering (DLS) spectrometer in an aqueous dispersion (Figure S1a). The thermal gravimetric analysis (TGA) of the nanomagnetic solid acid catalyst was carried out on a Shimadzu Thermogravimetric Analyzer (TG-50) in the temperature range of 25°C–900°C at a heating rate of 10°C/min in the air under N_2 atmosphere.

2.1.2 | Chemistry

*Typical experimental procedure for the synthesis of butyl 2-oxoacetate (**I**)*

Butyl 2-oxoacetate (**I**) was prepared according to a previously reported method (Scheme 1). In the first step, oxidation of dibutyl 2,3-dihydroxysuccinate (90 mmol: 25 g) with sodium metaperiodate solution (0.201 M, 150 ml) and then ether extraction led to 9.37 g (80% yields) of butyl 2-oxoacetate (**I**) (b.p. 55°C).[5,26]

*Typical experimental procedure for the synthesis of 2-chloroquinoxaline (**III**)*

2-Chloroquinoxaline (**III**) was prepared according to a previously reported method (Scheme 1). Freshly distilled phosphorus oxychloride $POCl_3$ (10 ml) was added slowly dropwise to quinoxalin-2-ol (**II**) (10.26 mmol: 1.5 g) at 0°C, and a few drops of dimethylformamide (DMF) were added to the mixture and refluxed for 12 h. Excess $POCl_3$ was distilled under reduced pressure, and the residue was cooled to room temperature and added to crushed ice. Then, the crude mixture was made alkaline by adding 2% NaOH solution and extracted with dichloromethane to isolate the product 2-chloroquinoxaline (**III**) (m.p. 48°C, 60% yields).[27] It seems necessary to mention that, in this study, quinoxalin-2-ol (**II**) was prepared through the catalytic procedure, as shown in Scheme 4.

*Typical experimental procedure for the synthesis of 2-(piperazin-1-yl) quinoxaline (**IV**)*

2-(Piperazin-1-yl) quinoxaline (**IV**) was prepared according to a previously reported method[28,29] (Scheme 1). A total of 3 mmol (0.4 g) of resulting 2-chloroquinoxaline (**III**) is taken up in toluene (10 ml), and this solution is then added dropwise to a refluxing solution of piperazine (6.9 mmol: 0.6 g) in 40 ml of toluene. The resulting light brown solution was refluxed for an additional 24 h and then cooled to 0°C for 30 min, filtered, and concentrated. The filtrate was extracted with 10% acetic acid, and the aqueous extracts were washed with ether and then basified and extracted with toluene. The toluene layer is washed with water, dried, and concentrated. The concentrated material was placed under vacuum overnight, and the product 2-(piperazin-1-yl) quinoxaline (**IV**) was obtained as a yellow solid (m.p. 74°C–76°C, yields 40%).

*Typical experimental procedure for the synthesis of 2-(chloromethyl)-1H-benzo[d]imidazole (**I′**)*

According to the literature review and reported methods (Scheme 2), a mixture of o-phenylenediamine (OPD; 9.5 mmol: 1.2 g) and chloroacetic acid (9.5 mmol: 0.9 g) was stirred in the presence of 4 N HCl (50 ml) at room temperature for approximately 3 h and then heated under reflux condition for several hours.[28] Then, the reaction mixture was cooled at room temperature, and the pH was adjusted to 9 by adding NH_4OH solution. The obtained precipitate was collected by filtration, washed with water, dried, and recrystallized from ethanol. The pure product was a slightly yellow-colored solid whose

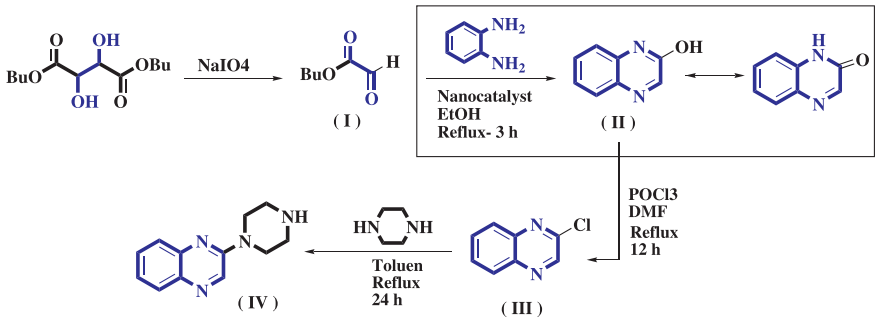

SCHEME 1 Typical experimental procedure for the synthesis of quinoxaline-based intermediate compound **IV**

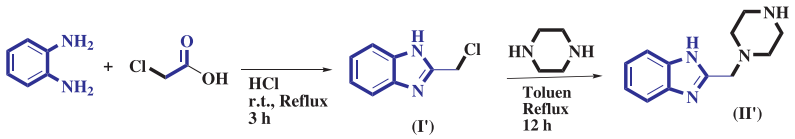

SCHEME 2 General experimental procedure for the synthesis of the benzimidazole-based intermediate compound **II′**

melting point was approximately 150°C, and the yield was 90%.

*Typical experimental procedure for the synthesis of 2-(piperazin-1-ylmethyl)-1H-benzo[d]imidazole (**II′**)*

A mixture of 1.66 g (0.01 m) of 2-(chloromethyl)-1*H*-benzo[d]imidazole (**I′**) was treated with excessive amounts of piperazine (0.05 m) in toluene (30 ml). The solution was stirred and gently heated overnight.[29] After completion of the reaction (monitored by TLC), the workup procedure was the same as 2-(piperazin-1-yl) quinoxaline (**IV**). The desired product 2-(piperazin-1-ylmethyl)-1*H*-benzo[d]imidazole (m.p. 248°C–251°C) was a pale-yellow solid in yield 80%.

2.2 | Stepwise synthesis of Fe_3O_4@PFBA–metformin@SO_3H nanocatalyst

In the first step, the Fe_3O_4 MNPs were synthesized by the coprecipitation method.[11] Afterward, 2.15 mmol (0.5 g) of the prepared Fe_3O_4 MNPs was well dispersed by ultrasonic vibration in 30 ml of methanol. Then PFBA at a concentration of 2.5 mmol/ml was added to the reaction mixture, which was stirred under reflux conditions overnight. The reaction mixture was cooled down, and the obtained Fe_3O_4@PFBA was separated by magnetic decantation and washed with methanol several times to remove the remaining impurities and dried in an oven at 80°C overnight.

In the next step, in order to synthesize Fe_3O_4@PFBA-metformin, 0.5 g of the prepared Fe_3O_4@PFBA MNPs was dispersed in 40 ml of methanol by sonication for 30 min, and then the solution of metformin hydrochloride (7.7 mmol in 20 ml of methanol) was added dropwise to the prepared suspension. The final suspension was stirred under reflux conditions for 2 h. Subsequently, the resultant Fe_3O_4@PFBA-metformin was collected by the magnet and washed with water–methanol (1:2) solution and then dried in an oven at about 80°C overnight.

Finally, to prepare the Fe_3O_4@PFBA–metformin@SO_3H catalytic organic–inorganic hybrid, 0.5 g of Fe_3O_4@PFBA-metformin MNPs was added in dry dichloromethane (10 ml) for 30 min. Then, chlorosulfonic acid (0.5 ml) was added dropwise at room temperature to the cooled (ice-batch) suspension of Fe_3O_4@PFBA-metformin (Scheme 3). Then, the final Fe_3O_4@PFBA–metformin@SO_3H MNPs were isolated—after the elimination of residual HCl by vacuum pressure—using an external magnet, washed by dichloromethane several times, and, finally, dried in an oven at 70°C.

2.3 | Typical experimental procedure for the synthesis of quinoxalin-2-ol in the presence of Fe_3O_4@PFBA–metformin@SO_3H nanocatalyst

Butyl 2-oxoacetate as our initial reagent was prepared according to a previously reported method.[26] In the second step, a mixture of butyl 2-oxoacetate (**I**) (100 mmol: 13 g) and OPD (100 mmol: 10.8 g) with a molar proportion of 1:1, in the presence of Fe_3O_4@PFBA–metformin@SO_3H (40 mg), was dissolved in absolute ethanol (20 ml) and then stirred at reflux conditions. The progress of the reaction was monitored by TLC. After completion of the reaction (in approximately 2 h), the

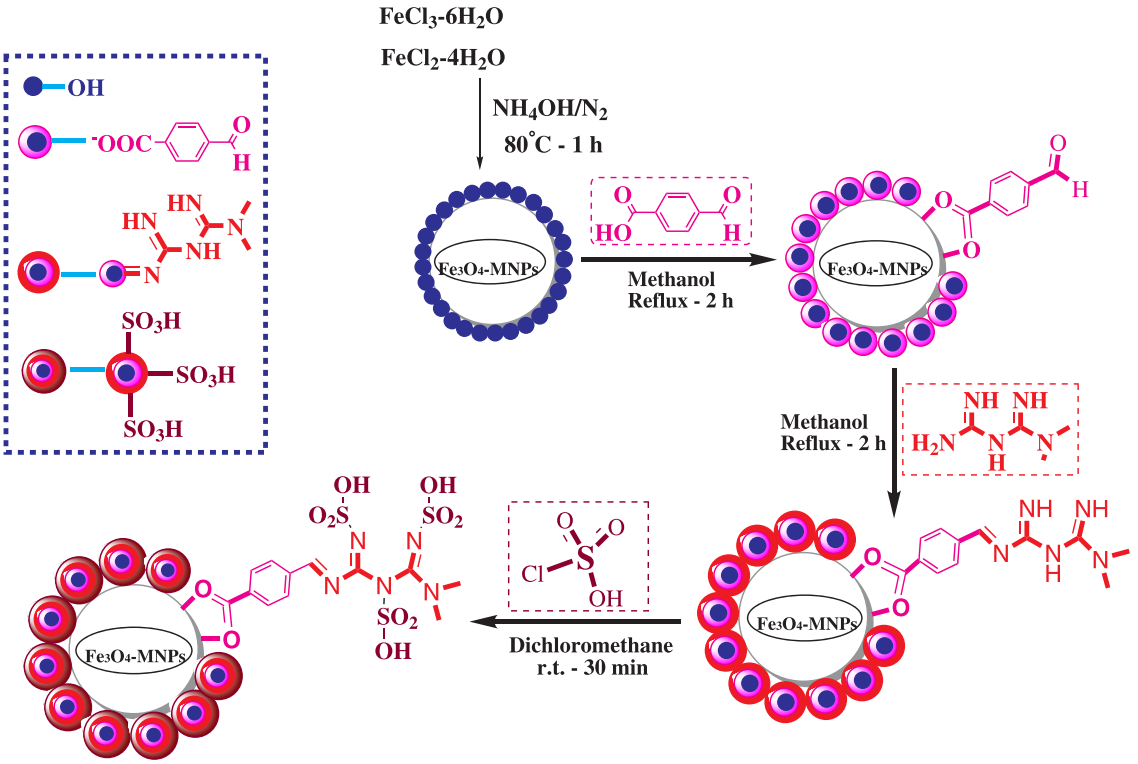

SCHEME 3 Preparation of the Fe_3O_4@PFBA–metformin@SO_3H nanocatalyst

SCHEME 4 Synthesis of quinoxaline-2-ol

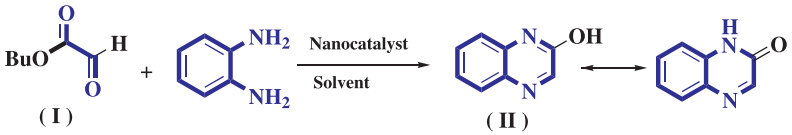

catalyst was separated from the reaction mixture by a simple external magnet, and the product quinoxalin-2-ol (**II**) was obtained by concentration and filtration in 90% yield and no need for purification process (m.p. 268–272).

2.4 | General procedure for the synthesis of N-Mannich bases 6a–6d and 4′a–4′d from secondary amine-containing compounds (IV, II′) in the presence of Fe_3O_4@PFBA–metformin@SO_3H as nanocatalyst

In the presence of Fe_3O_4@PFBA–metformin@SO_3H MNPs (40 mg), a solution of (substituted) isatin (1 mmol) in 5 ml of absolute ethanol was added to equimolar amounts of aqueous formaldehyde 37% in 10 ml absolute ethanol and 2-(piperazin-1-yl) quinoxaline (**IV**) or 2-piperazin-1-ylmethyl-1*H*-benzoimidazole (**II'**) as our initial reagents, which were prepared according to the reported procedure (Schemes 1 and 2).[27] The prepared reaction mixture was stirred and refluxed for about 3 h to form the final products (**6a–6d** and **4′a–4′d**), and the progress of the reaction was monitored by TLC. Then, the nanocatalyst was separated from the reaction mixture by the magnetic field and washed with hot ethanol. Then, the reaction mixture was concentrated under vacuum, and an orange crystalline product appeared and was separated by filtration, washed, and vacuum dried.

2.5 | General procedure for the synthesis of Mannich bases 7a–7h, 5′a–5h, 8a–8d, and 6′a–6′d secondary amine-containing compounds (IV, II′) using Fe_3O_4@PFBA–metformin@SO_3H

A mixture of 1 mmol (0.2 g) piperazinyl containing core 2-(piperazin-1-yl) quinoxaline (**IV**) or 2-piperazin-1-ylmethyl-1*H*-benzoimidazole (**II′**), formaldehyde 37% (1 mmol), (substituted) isatin (1 mmol), and

amine-containing tail portion thio/semicarbazide or metformin (1 mmol) in the presence of Fe_3O_4@PFBA–metformin@SO_3H MNPs (40 mg) was dissolved in absolute ethanol and stirred at reflux conditions for 2 h. The progress of the reaction was monitored by TLC (chloroform:methanol, 9:1). Then, the nanocatalyst was separated from the reaction mixture by an external magnet and washed with hot ethanol, and the products were obtained from the reaction solution under reduced pressure and recrystallized from a mixture of solvent hexane/chloroform.

2.6 | General procedure for Fe_3O_4@PFBA–metformin@SO_3H catalyzed synthesis of (substituted) isatin derivatives (CO_1–CO_{12})

A mixture of (substituted) isatin (1 mmol) with equimolar amounts of thio/semicarbazide or metformin (1,1-dimethylbiguanide) in the presence of Fe_3O_4@PFBA–metformin@SO_3H MNPs (40 mg) was dissolved in absolute ethanol and stirred at reflux conditions for 150 min up to 3 h. The progress of the reaction was monitored by TLC (chloroform:methanol, 9:1). Then, the nanocatalyst was separated from the reaction mixture by an external magnet and washed with hot ethanol. The (substituted) isatin-3-thio/semicarbazones and isatin-3-1,-1-dimethylbiguanide derivatives (CO_1– CO_{12}) were obtained from the reaction solution simply under reduced pressure.

2.7 | Selected spectral data

The analytical and spectroscopic data (^{1}H NMR, ^{13}CNMR, and FTIR) for the unknown final products (**6a–6d**, **7a–7h**, **8a–8d**, **4′a–4′d**, and **5′a–5′h**) are available in the supporting information (Figures S1–S157).

3 | RESULTS AND DISCUSSION

3.1 | Nanocatalyst preparation

In this work, a novel sulfamic acid supported on Fe_3O_4 was prepared, as shown in Scheme 3. In order to prepare the Fe_3O_4@PFBA magnetic nanocatalyst, PFBA has been grafted on Fe_3O_4 MNPs via the covalent bonding of R-COOH groups with OH groups under the surface of Fe_3O_4 MNPs. The metformin was grafted on Fe_3O_4@PFBA MNPs by a Schiff base reaction; finally, the catalyst was synthesized by the reaction of Fe_3O_4@PFBA-metformin MNPs with chlorosulfonic acid (Scheme 3).

3.2 | Nanocatalyst characterizations

After the synthesis of Fe_3O_4@PFBA–metformin@SO_3H MNPs, its structure was fully characterized by FTIR, XRD, EDX, field-emission SEM (FESEM), TEM, AFM, TGA, VSM, Brunauer–Emmett–Teller (BET) (Figure S1a), and DLS (Figures S1b) analyses. The characterization results confirmed the successful synthesis of the nanocatalyst.

The FTIR spectra of Fe_3O_4 MNPs, Fe_3O_4@PFBA MNPs, Fe_3O_4@PFBA-metformin MNPs, and Fe_3O_4@PFBA–metformin@SO_3H nanocatalyst are shown in Figure 1. The FTIR spectrum of Fe_3O_4 MNPs shows a particular IR band in the area of 585 cm^{-1}, and a broadband around 3,386 cm^{-1} is due to O–H stretching of adsorbed water. In the FTIR spectrum of Fe_3O_4@PFBA, the COO–Fe, C–H, C–O, C═O groups, and Fe–O band at 1,647, 3,445, 1,233, 1,681, and 651 cm^{-1} regions, respectively, confirmed the successful immobilization of PFBA ligand on the surface of the Fe_3O_4 support. In the FTIR spectrum of Fe_3O_4@PFBA-metformin MNPs, the band located around 3,000 cm^{-1} is related to C–H stretching, whereas the bands observed at 3,350 and 1,500 cm^{-1} correspond to N–H stretching. The

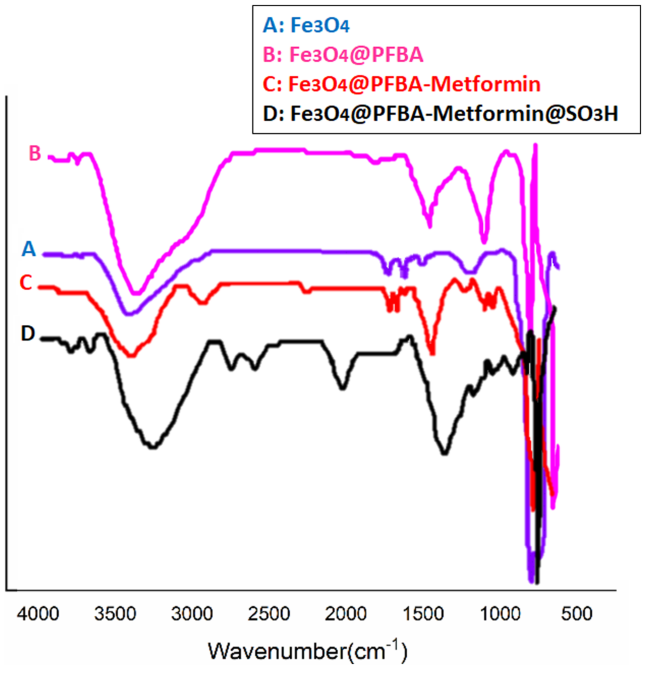

FIGURE 1 Fourier transform infrared (FTIR) spectra of Fe_3O_4 magnetic nanoparticles (MNPs), Fe_3O_4@PFBA MNPs, Fe_3O_4@PFBA-metformin MNPs, Fe_3O_4@PFBA–metformin@SO_3H MNPs

distinguishing feature of the Fe_3O_4@PFBA–metformin@SO_3H (Figure 1) is the presence of new bands at 1,070 and 1,040 cm^{-1} in the spectrum, which are ascribed to the typical symmetric stretching of the S═O bond. The S═O bond intensity is fairly weak in the IR spectra, basically because the sulfur content is quite low in the total unit. The strong peak at 580 cm^{-1} indicates the presence of magnetite in the products; in addition, the consequences show a good agreement between FTIR of the fresh (Figure 1) and spent catalyst (Figure 10). Therefore, Figure 10 indicates the good stability of Fe_3O_4@PFBA–metformin@SO_3H after recycling.

In order to investigate the crystallographic features of the prepared nanocatalyst, an XRD analysis of the samples was performed. As shown in Figure 2, the synthesis of Fe_3O_4@PFBA-metformin MNPs with SO_3H MNPs was justified by the XRD peak positions at 2θ = 30.86°, 35.356°, 43.96°, 53.36°, 57.26°, and 62.56°, which are related to (220), (311), (400), (422), (511), and (440) reflections, respectively. This pattern was consistent with the standard XRD data for bulk Fe_3O_4 (JCPDS, card 19-0629). This analysis clearly affirmed that the surface modification and functionalization of the Fe_3O_4 nanoparticles did not lead to phase change. The XRD pattern of the recycled catalyst is shown in Figure 2. The results show that a good agreement was observed for XRD of the fresh Fe_3O_4@PFBA-metformin, Fe_3O_4@PFBA–metformin@SO_3H MNPs (Figure 2), and the recycled nanocatalyst (Figure 10). Therefore, the XRD results indicate the good stability of Fe_3O_4@PFBA–metformin@SO_3H MNPs after recycling.

The element composition of the synthesized Fe_3O_4@PFBA–metformin@SO_3H nanostructure was studied using EDX and elemental mapping, which showed the presence of Fe, O, C, N, and S species in the prepared nanocatalyst (Figure 3a,b). The results confirmed the mentioned successful immobilization of the sulfamic acid catalytic complex on the surface of Fe_3O_4 MNPs (Figure 3a). Moreover, in order to find the stability of the elements of catalyst, EDS analysis of the recycled Fe_3O_4@PFBA–metformin@SO_3H was conducted. Compared with that of the fresh catalyst (Figure 3a vs. Figure 10), the EDS spectrum of the spent catalyst shows the existence of Fe, O, C, N, and S species. Therefore, the element composition of the catalyst has not been changed after several times of recycling.

In order to evaluate the morphology and particle size of the Fe_3O_4@PFBA–metformin@SO_3H magnetic nanocatalyst, SEM was used (Figure 4). On the basis of SEM images, some catalytic particles in the Fe_3O_4@PFBA–metformin@SO_3H sample are round-shaped particles with diameters of about 20 nm. In addition, in order to indicate the stability of the catalyst during organic reactions, its morphology after the catalytic test was evaluated by the SEM technique (Figure 4). As shown in Figure 4, the spent catalyst size and morphology are good agreement with the fresh catalyst (Figure 4). Therefore, the SEM analysis indicates the good stability of Fe_3O_4@PFBA–metformin@SO_3H nanocatalyst after recycling.

The size and morphology of the synthesized Fe_3O_4@PFBA–metformin@SO_3H were further evaluated by high-resolution TEM, which shows simply a well-defined core–shell structure with a shell thickness of about 50 nm (Figure 5). The SEM and TEM images also confirmed that the Fe_3O_4@PFBA-metformin and Fe_3O_4@PFBA–metformin@SO_3H MNPs were so stable that the sulfonating and catalytic processes were not able to decay the structures and morphologies of PFBA-metformin MNPs. These factors enabled the Fe_3O_4@PFBA–metformin@SO_3H MNPs to meet the demands for highly efficient, magnetically separable, and stable solid (heterogeneous) acid nanocatalyst.

The thermal stability of Fe_3O_4@PFBA–metformin@SO_3H was studied using TGA (Figure 6). The first small weight loss taking place below 100°C is due to the solvent desorption. The second weight loss can be ascribed to the decomposition of the organic fragment. As the TGA curve shows, the amount of the organic compound was around 5.5% versus the total catalyst. Because of that weight loss, it was found that 0.71 mmol of the organic component was loaded on 1 g of Fe_3O_4@PFBA–metformin@SO_3H nanocatalyst. The TGA curve of the catalyst Fe_3O_4@PFBA–metformin@SO_3H reveals the loss of the organic functional groups as it decomposes upon heating. The weight loss at temperatures below 230°C for

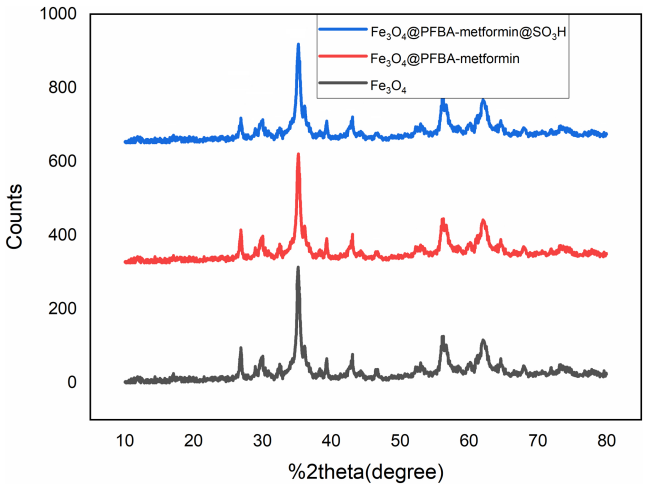

FIGURE 2 X-ray diffraction (XRD) patterns of Fe_3O_4, fresh nanocatalyst Fe_3O_4@PFBA-metformin magnetic nanoparticles (MNPs), and Fe_3O_4@PFBA–metformin@SO_3H nanocatalyst

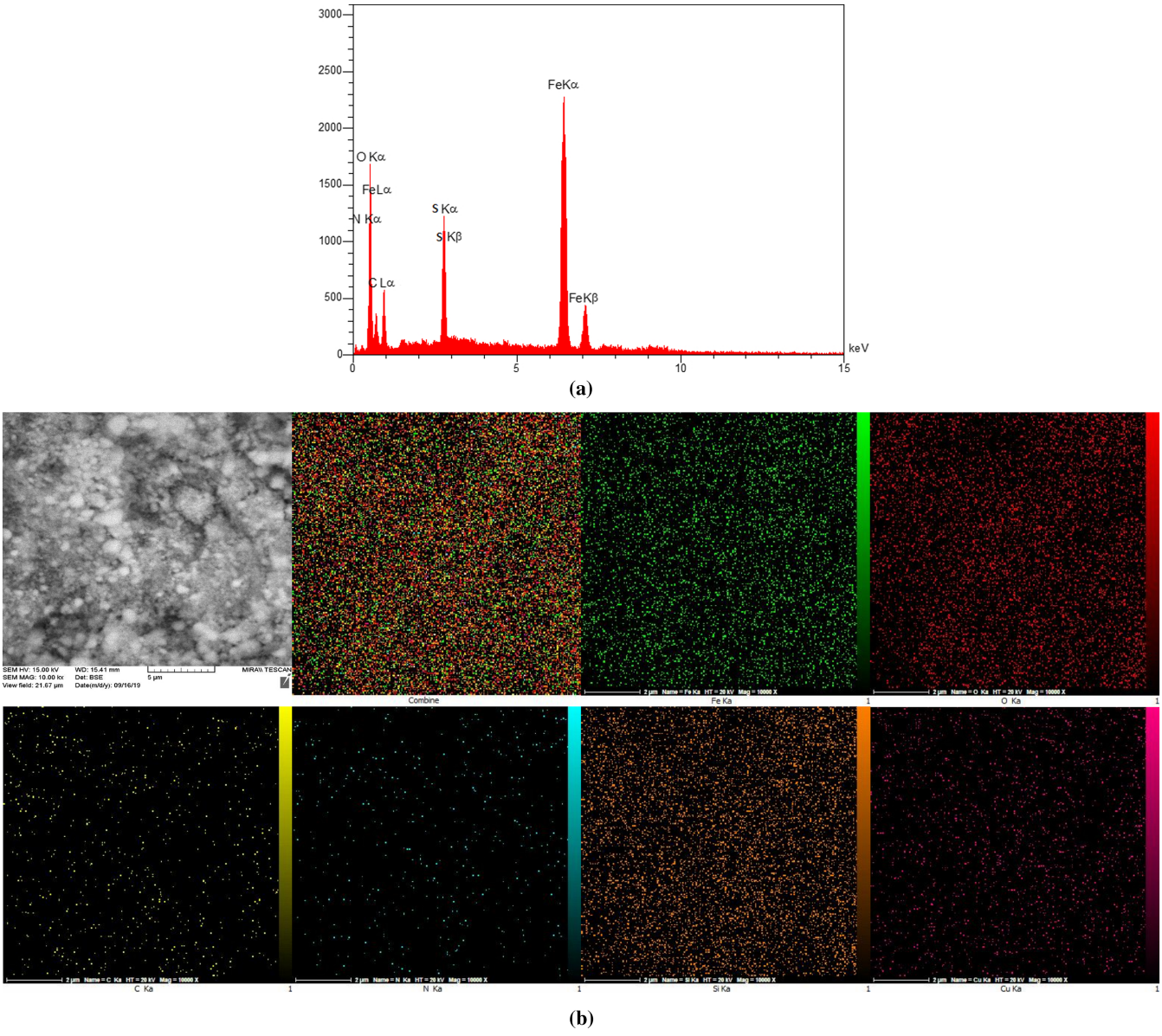

FIGURE 3 (a) Energy-dispersive X-ray spectroscopy (EDX) spectrum of Fe_3O_4@PFBA–metformin@SO_3H and (b) EDX elemental mapping of the nanocatalyst Fe_3O_4@PFBA–metformin@SO_3H

the sample is due to the loss of adsorbed water or the water that is formed by the condensation of hydroxyl groups. Some weight loss at around 230°C–650°C is due to the evaporation and disintegration of organic groups attached to the surface of Fe_3O_4 MNPs. Thus, according to the TGA curve, the amount of organic and inorganic moieties was around 5.5% and 3.5% against the total heterogeneous catalyst, respectively.[26]

To evaluate the magnetic properties of Fe_3O_4@PFBA-metformin and Fe_3O_4@PFBA–metformin@SO_3H, a VSM sample was used in an applied field of approximately 10,000 Oe at room temperature. According to the VSM results (Figure 7), the amount of saturated magnetic resonance (MS) for Fe_3O_4@PFBA-metformin and Fe_3O_4@PFBA–metformin@SO_3H acidic nanocatalyst is approximately 51 and 47 emu/g, respectively. The MS for Fe_3O_4@PFBA-metformin and Fe_3O_4@PFBA–metformin@SO_3H have a significant decrease compared with uncoated Fe_3O_4MNPs (67.22 emu/g) due to the increase in the amount of organic compounds on the surface of MNPs.[25–27]

Figure 8 shows the AFM image of the synthesized nanocatalyst Fe_3O_4@PFBA–metformin@SO_3H. The AFM micrograph confirms the surface roughness after the functionalization of Fe_3O_4 with PFBA-metformin@SO_3H.

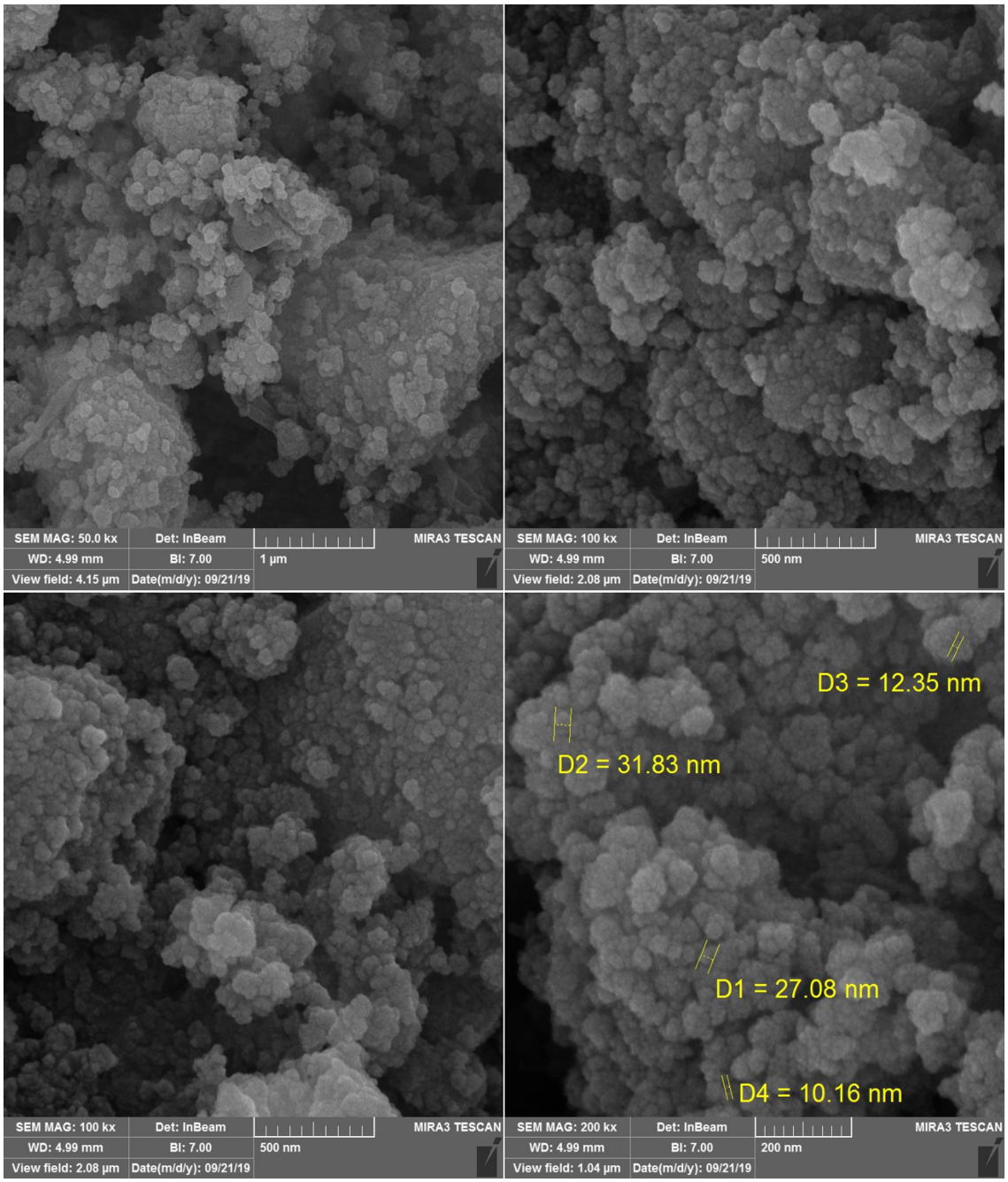

FIGURE 4 Scanning electron microscopy (SEM) images of Fe_3O_4@PFBA–metformin@SO_3H (a) recovered nanocatalyst after catalysis (b)

3.3 | Catalytic study

After characterizing the synthesized Fe_3O_4@PFBA–metformin@SO_3H, its catalytic activity was evaluated in four synthetic procedures (including cyclocondensation, condensation, and Mannich reaction).

Initially, the catalytic properties of Fe_3O_4@PFBA–metformin@SO_3H were examined in the synthesis of quinoxaline-2-ol (Scheme 4). To find the best reaction conditions, the effect of the different experimental parameters (e.g., the effects of solvent, catalyst amounts, and temperature) on the reaction efficiency was studied (Table 1). The highest yields were obtained in the presence of 40 mg of Fe_3O_4@PFBA–metformin@SO_3H. Evidently, with the lack of the catalyst, the reaction could not progress by 24 h (Table 1, Entry **1**). After a wide screening, the highest yield, best reaction time, and reduction of undesired side products were obtained when the reaction was supported in the presence of 40 mg of the newly synthesized nanocatalyst

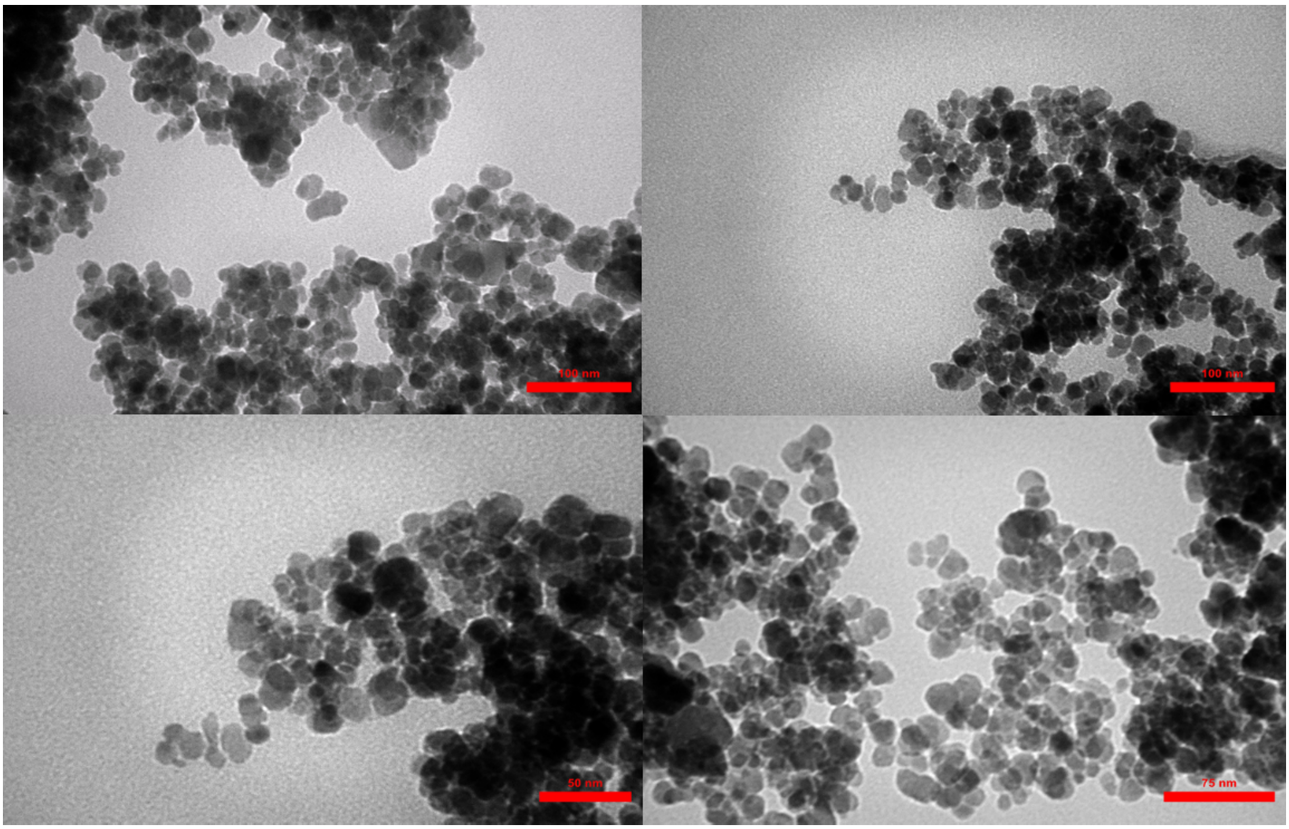

FIGURE 5 Transmission electron microscopy (TEM) images of Fe_3O_4@PFBA–metformin@SO_3H

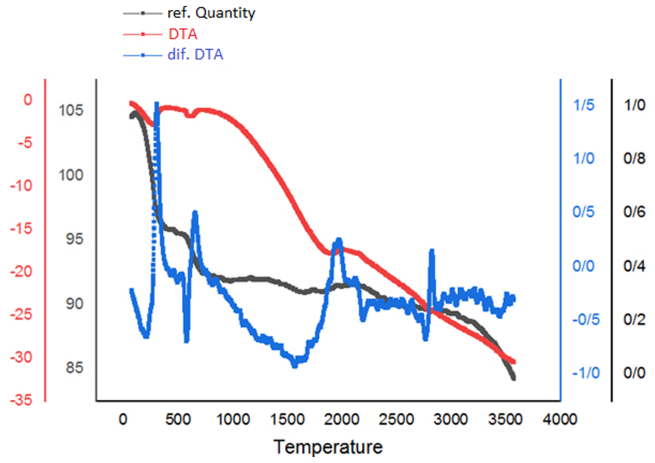

FIGURE 6 Thermogravimetric analysis (TGA) curve of Fe_3O_4@PFBA–metformin@SO_3H

under reflux conditions in absolute ethanol as a benign and green solvent.

The catalytic activity of Fe_3O_4@PFBA–metformin@SO_3H nanocatalyst has also been investigated in the reaction of a three-component coupling of 2-(piperazin-1-yl) quinoxaline (**IV**) (1 mmol), formaldehyde (37%), and isatin (1 mmol) as our first model reaction (Table 2). The effects of reaction temperature, catalyst amount, and solvent were examined to optimize the reaction parameters. The reaction was performed in the absence of the nanocatalyst, and poor results were obtained. Different amounts of Fe_3O_4@PFBA–metformin@SO_3H were studied at 50°C and 100°C in (absolute) ethanol as a benign polar and protic solvent, and the product yields increased from 38% to 95% by increasing the catalyst loading from 10 to 40 mg (Table 2, Entries **4**–**8**). However, no changes in yields were observed when the amounts of the nanocatalyst increased to 80 mg (Table 2, Entry **9**). Reaction yields generally decreased, as expected, with a temperature decrease. In absolute ethanol, the serious problem of unwanted by-products was less annoying compared to ethanol. These were considered as optimum conditions for this kind of three-component reaction (Table 2, Entry **8**).

After finding the optimum reaction conditions in the presence of the nanocatalyst, we employed different substituted isatins for similar three-component reactions, and Fe_3O_4@PFBA–metformin@SO_3H provided excellent yields for the corresponding final products in all reactions. The results are summarized in Scheme 5 and Table 3.

We have studied the catalytic activity of Fe_3O_4@PFBA–metformin@SO_3H nanoparticles for the synthesis of Mannich Schiff bases of isatin between

different substituted isatins and amine containing terminal groups (thio/semicarbazide and metformin; Scheme 6). In order to optimize the reaction conditions, isatin (1 mmol) and semicarbazide (1 mmol) were used as the model reaction in several different conditions such as different amounts of the nanocatalyst (5, 10, and 15 mg), temperature, time, and solvent. The optimal conditions of the reaction were selected to use absolute ethanol as solvent, under reflux condition, and in the presence of 40 mg Fe_3O_4@PFBA–metformin@SO_3H nanocatalyst (Table 4, Entry **11**). The results showed no substantial improvement in the yield with a further increase of the nanocatalyst.

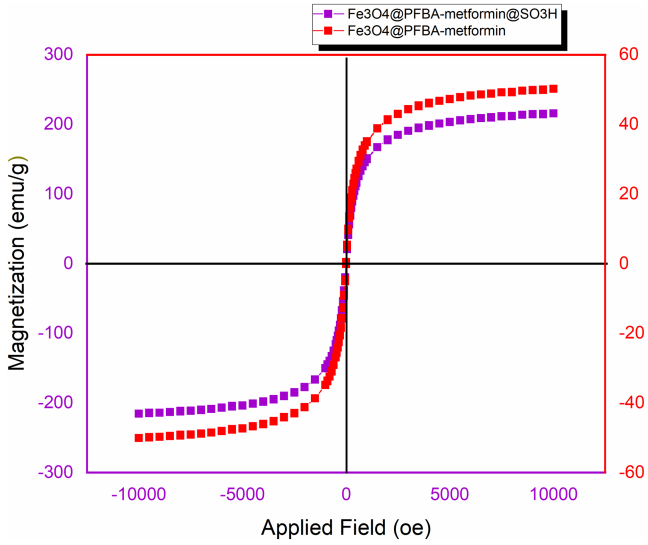

FIGURE 7 Vibrating sample magnetometer (VSM) of fresh Fe_3O_4@PFBA–metformin and Fe_3O_4@PFBA–metformin@SO_3H

With the optimized reaction conditions, different substituted isatins and thio/semicarbazide or metformin gave desired products in good yields (92%–99%) in 150 min (Table 5). The typical results of the above-mentioned Fe_3O_4@PFBA–metformin@SO_3H-catalyzed Mannich reactions, under optimized conditions, are shown below in Scheme 6 and Table 5.

In order to improve the reaction parameters, the condensation of 2-(piperazin-1-yl) quinoxaline (**IV**) (1 mmol), formaldehyde (37%), isatin, and semicarbazide (1 mmol) was performed to afford compound **7a**. The results are shown in Table 6. According to optimization studies, absolute ethanol was presented

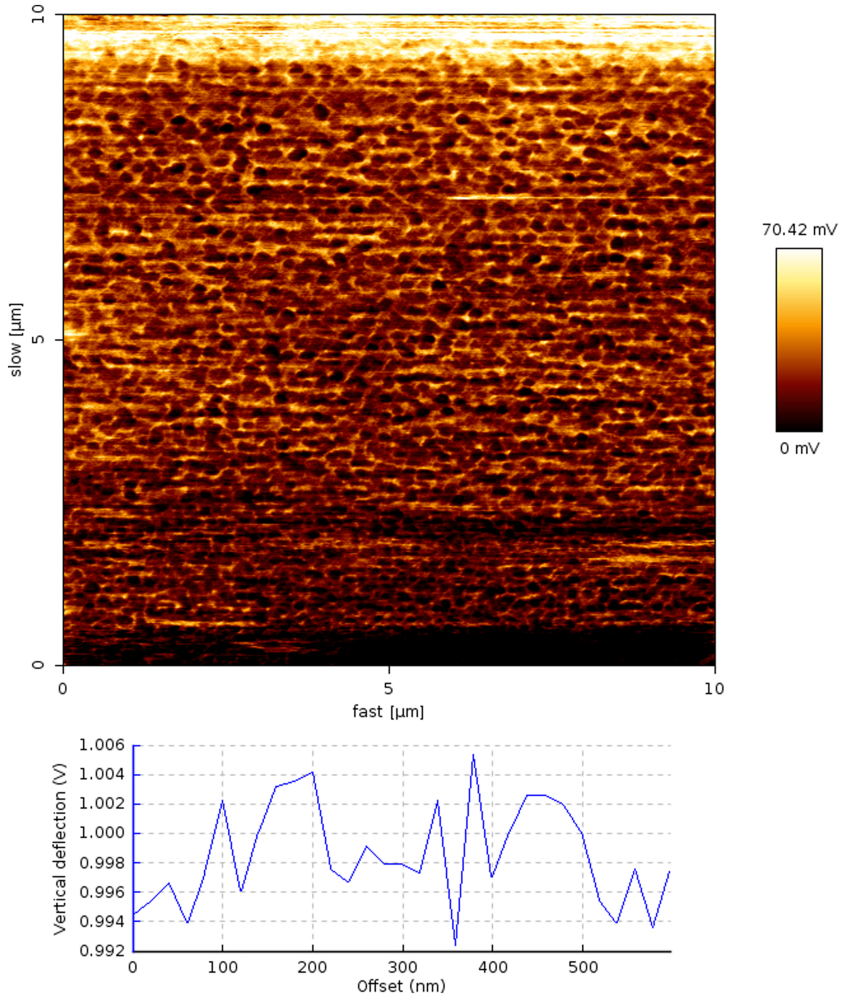

FIGURE 8 Atomic force microscopy (AFM) image of the Fe_3O_4@PFBA–metformin@SO_3H nanocatalyst

TABLE 1 Optimizing the reaction conditions for the cyclocondensation of OPD with butyl 2-oxoacetate (**I**): production of compound **II**[a]

Entry	Catalyst (g)	Solvent	Temperature (°C)	Time (h)	Yield (%)[b]
1	—	Ethanol	Reflux	24	—
2	PFBA or metformin	Ethanol	Reflux	24	—[c]
3	Fe_3O_4@PFBA-metformin	Ethanol, water	Reflux	24	—
4	Fe_3O_4 MNPs (50 mg)	Ethanol	Reflux	24	20
5	Fe_3O_4@PFBA–metformin@SO_3H (10 mg)	Ethanol, water	r.t.	8	Trace
6	Fe_3O_4@PFBA–metformin@SO_3H (10 mg)	Ethanol	Reflux	3	35
7	Fe_3O_4@PFBA–metformin@SO_3H (10 mg)	Water	Reflux	3	20
8	Fe_3O_4@PFBA–metformin@SO_3H (20 mg)	Ethanol	Reflux	3	50
9	Fe_3O_4@PFBA–metformin@SO_3H (30 mg)	Ethanol	Reflux	3	67
10	Fe_3O_4@PFBA–metformin@SO_3H (40 mg)	Ethanol	Reflux	3	90
11	Fe_3O_4@PFBA–metformin@SO_3H (60 mg)	Ethanol	Reflux	3	90

[a]Reaction conditions: Butyl 2-oxoacetate (1 mmol), OPD (1 mmol), and catalyst in the solvent,
[b]Isolated yield.
[c]Unwanted by-products.

TABLE 2 Model reaction 1: Optimizing the model reaction conditions for the synthesis of the compound **6a**[a]

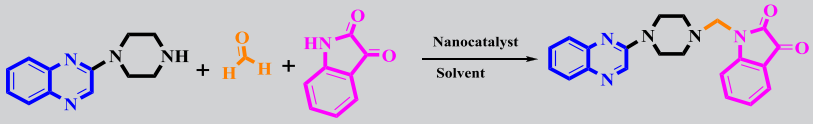

Entry	Catalyst (g)	Solvent	Temperature (°C)	Time (h)	Yield (%)[b]
1	—	Ethanol	50, Reflux	24	—
2	Nano-Fe_3O_4 (50 mg)	Ethanol	50, Reflux	24	—
3	Nanocatalyst (10 mg)	Ethanol	Reflux	3	38
4	Nanocatalyst (10 mg)	Ethanol	50	24	—
5	Nanocatalyst (10 mg)	Absolute ethanol	Reflux	3	45
6	Nanocatalyst (20 mg)	Absolute ethanol	Reflux	3	60
7	Nanocatalyst (30 mg)	Absolute ethanol	Reflux	3	75
8	Nanocatalyst (40 mg)	Absolute ethanol	Reflux	3	95
9	Nanocatalyst (80 mg)	Absolute ethanol	Reflux	3	95
10[c,d]	GAA (a few drops)	Ethanol	Reflux	Overnight	Trace
11	GAA (a few drops)	Absolute ethanol	50	Overnight	—
12	Recovered nanocatalyst	Absolute ethanol	Reflux	3	95

[a]Reaction conditions: 2-(piperazin-1-yl) quinoxaline (**IV**) (1 mmol), formaldehyde (1 mmol), isatin (1 mmol), and catalyst in the solvent.
[b]Isolated yield after recrystallization,
[c]Hard workup.
[d]Unwanted by-product.

as the best solvent with its high yield, green character, cheapness, and eco-friendly nature. Also, higher catalyst amounts did not affect the yield significantly. Accordingly, the optimum conditions for this one-pot protocol are summarized in Table 6, Entry **10** (95% yield).

The variety of (substituted) isatins and amine-containing compounds (thio/semicarbazide and

SCHEME 5 Synthesis of 2-piperazinyl quinoxaline and 2-piperazin-1-ylmethyl-1*H*-benzoimidazole derivatives (**6a–6d** and **4′a–4′d**) by Fe_3O_4@PFBA–metformin@SO_3H

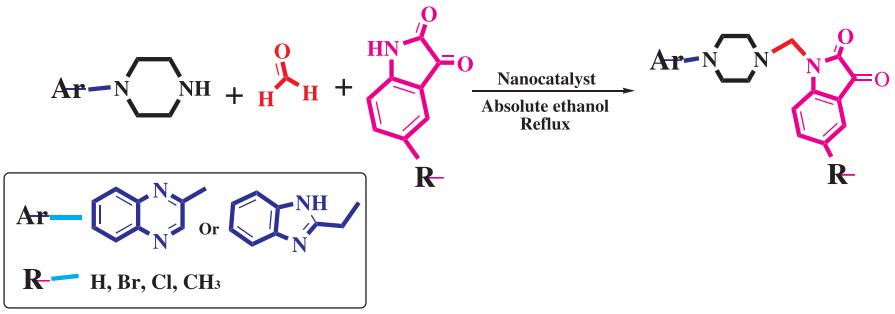

TABLE 3 Fe_3O_4@PFBA-metformin@sulfonic acid-catalyzed reaction of 2-piperazinyl quinoxaline or 2-(piperazin-1-ylmethyl)-benzimidazole with formaldehyde and various isatin derivatives under optimized reaction conditions

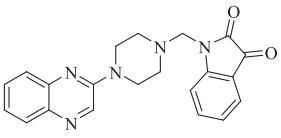

6a
Yield (95%)
m.p. 180 °C

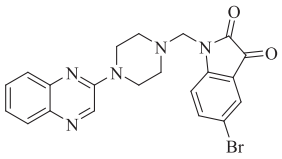

6b
Yield (99%)
m.p. 144 °C

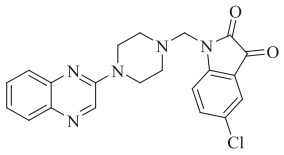

6c
Yield (98%)
m.p. 191 °C

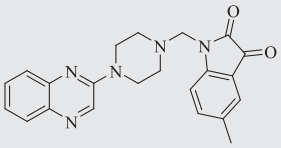

6d
Yield (95%)
m.p. 178°C–185°C

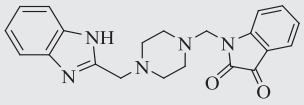

4′a
Yield (90%)
m.p. 160°C

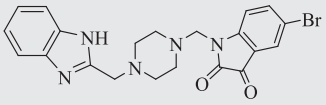

4′b
Yield (98%)
m.p. 140°C

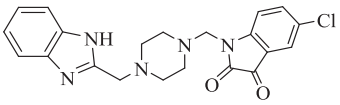

4′c
Yield (98%)
m.p. 180°C

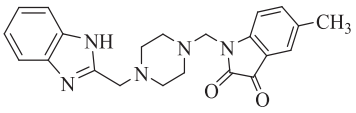

4′d
Yield (95%)
m.p. 170°C

metformin) was used as the reaction substrates to produce corresponding Schiff Mannich bases under the optimized reaction conditions in the presence of Fe_3O_4@PFBA–Metformin@SO_3H at reflux temperature for about 3 h (90%–99% yields). The results are depicted in Scheme 7 and Table 7.

Although the exact mechanism of this procedure is not crystal clear, one of the suggested reaction pathways for the Mannich reaction in the presence of Fe_3O_4@PFBA–metformin@SO_3H as a heterogeneous Lewis acid catalyst is outlined in Scheme 8. Electron-deficient sites on the surface of the heterogeneous nanocatalyst Fe_3O_4@PFBA–metformin@SO_3H could coordinate with the O-donor sites of formaldehyde and (substituted) isatin. The electrophilicity of the carbonyl carbon atom of both formaldehyde and isatins

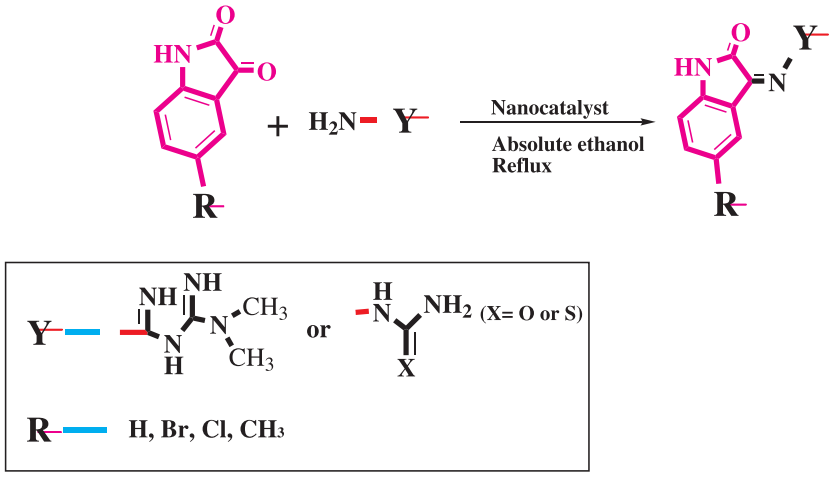

SCHEME 6 Synthesis of (substituted) isatin derivatives (CO_{1-12}) by Fe_3O_4@PFBA–metformin@SO_3H

TABLE 4 Model reaction 4: Optimizing the model reaction conditions for the synthesis of the compound CO_1

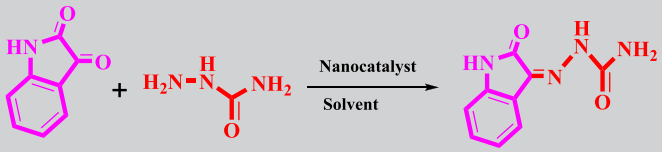

Entry	Catalyst (g)	Solvent	Temperature (°C)	Time	Yield[a] (%)[b]
1	—	(Absolute) ethanol	r.t.	24 h	—
2	—	(Absolute) ethanol	Reflux	8 h	Trace
3	Nano-Fe_3O_4 (50 mg)	(Absolute) ethanol	r.t.	24 h	—
4	Nano-Fe_3O_4 (50 mg)	(Absolute) ethanol	Reflux	8 h	—
5	Nano-Fe_3O_4 (100 mg)	(Absolute) ethanol	r.t., reflux	24 h	—
6	Nanocatalyst (10 mg)	(Absolute) ethanol	r.t.	8 h	15
7	Nanocatalyst (10 mg)	Ethanol	Reflux	5 h	30
8	Nanocatalyst (10 mg)	Absolute ethanol	Reflux	3 h	30
9	Nanocatalyst (20 mg)	Absolute ethanol	Reflux	3 h	45
10	Nanocatalyst (30 mg)	Absolute ethanol	Reflux	3 h	60
11	Nanocatalyst (40 mg)	Absolute ethanol	Reflux	150 min	95
12	Nanocatalyst (80 mg)	Absolute ethanol	Reflux	150 min	95
13	GAA (a few drops)	Ethanol	Reflux	Overnight	30[c,d]
14	GAA (a few drops)	Absolute ethanol	Reflux	Overnight	30

Note. All catalyzed reactions take up to 3 h.
[a]Reaction conditions: isatin (1 mmol) and smicarbazide (1 mmol).
[b]Isolated yield.
[c]Hard workup.
[d]Unwanted by-product.

enhances because of coordination with the empty orbital of $–SO_3H$ group at the surface of the functionalized Fe_3O_4.[30] Subsequently, the Mannich reaction leads to the corresponding Mannich base product.

3.4 | Recycling studies

The reusability of the catalyst was evaluated by the reaction of 2-(piperazin-1-yl) quinoxaline (**IV**) (1 mmol), formaldehyde (37%), and isatin (1 mmol; Model Reaction

TABLE 5 Fe_3O_4@PFBA–metformin@SO_3H-catalyzed reaction of substituted isatins and the amino-containing tail portion (semicarbazone, thiosemicarbazone, and *N*,*N*-dimethylbiguanide [metformin]) under optimized reaction conditions

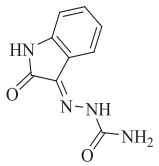	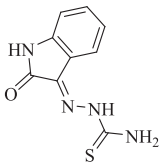	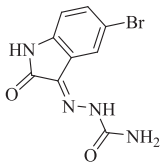
CO_1 Yield (95%) m.p. 270°C	CO_2 Yield (95%) m.p. 238°C–240°C	CO_3 Yield (98%) m.p. 269°C
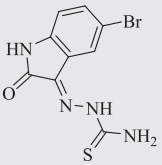	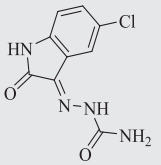	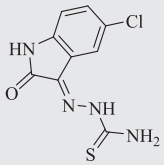
CO_4 Yield (98%) m.p. 240°C	CO_5 Yield (95%) m.p. 272°C	CO_6 Yield (99%) m.p. 245°C
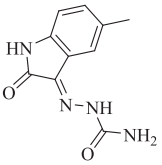	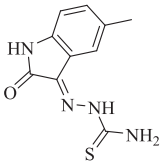	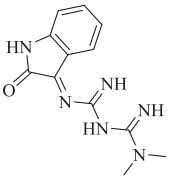
CO_7 Yield (90%) m.p. 275°C–280°C	CO_8 Yield (92%) m.p. 250°C	CO_9 Yield (90%) m.p. 185°C
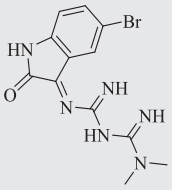	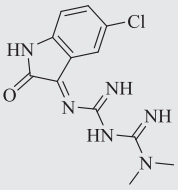	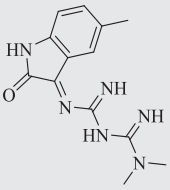
CO_{10} Yield (93%) m.p. 184°C–188°C	CO_{11} Yield (96%) m.p. 185°C	CO_{12} Yield (90%) m.p. 187°C

1) using catalyst Fe_3O_4@PFBA-metformine@SO_3H under optimized conditions (Table 2, Entry **8**). The catalytic activity of the recovered catalyst in the same reaction under optimized conditions shows that the magnetically separated nanocatalyst is reusable for six consecutive runs without any significant loss in catalytic activity (Figure 9).

To find reliable results, we employed the FTIR, SEM, XRD, and VSM techniques to analyze the recovered Fe_3O_4@PFBA–metformin@SO_3H nanocatalyst

TABLE 6 Model reaction 3: Optimizing the model reaction conditions for the synthesis of the compound **7a**[a]

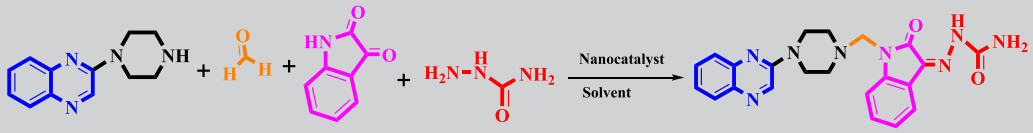

Entry	Catalyst[b] (g)	Solvent	Temperature (°C)	Time	Yield[a] (%)[c]
1[d]	—	Ethanol	r.t., reflux	48	—
2	Nano-Fe_3O_4 (50 mg)	Ethanol	r.t., reflux	48	—
3	Nano-Fe_3O_4 (100 mg)	Ethanol	r.t., reflux	48	—
4	Nanocatalyst (10 mg)	Ethanol	Reflux	3	40
5	Nanocatalyst (10 mg)	Ethanol	r.t.	24	Trace
6	Nanocatalyst (10 mg)	Absolute ethanol	Reflux	3	48
7	Nanocatalyst (10 mg)	H_2O	Reflux	24	—
8	Nanocatalyst (20 mg)	Absolute ethanol	Reflux	3	60
9	Nanocatalyst (30 mg)	Absolute ethanol	Reflux	3	65–70
10	Nanocatalyst (40 mg)	Absolute ethanol	Reflux	3	95
11	Nanocatalyst (40 mg)	Ethanol	Reflux	3	60
12	Nanocatalyst (40 mg)	Absolute ethanol	r.t.	10	Trace
13	Nanocatalyst (80 mg)	Absolute ethanol	Reflux	3	95
14	Nanocatalyst (80 mg)	Absolute ethanol	r.t.	10	Trace
15	GAA (a few drops)	Absolute ethanol	r.t.	Overnight	—
16	GAA (a few drops)	Absolute ethanol	Reflux	Overnight	Trace[d,e]
17	Recovered nanocatalyst	Absolute ethanol	Reflux	3	95

[a]Reaction conditions: 2-(piperazin-1-yl) quinoxaline (**IV**) (1 mmol), formalin (37%), isatin, and semicarbazide (1 mmol).
[b]Fe_3O_4@PFBA–metformin@SO_3H.
[c]Isolated yield after recrystallization.
[d]Unwanted by-product.
[e]Hard workup.

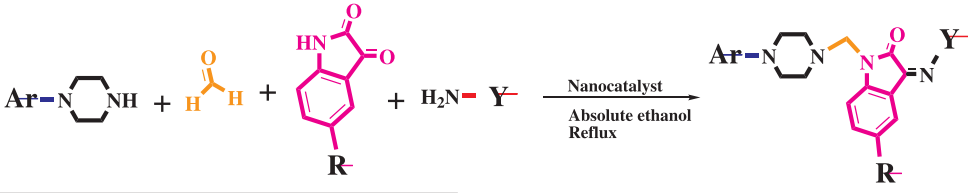

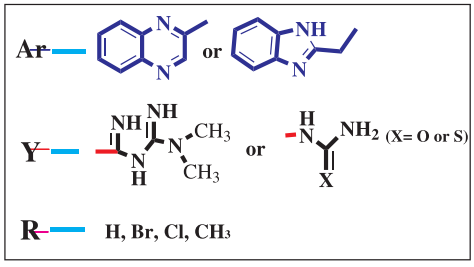

SCHEME 7 Synthesis of 2-piperazinyl quinoxaline and 2-piperazin-1-ylmethyl-1*H*-benzoimidazole derivatives (**7a–7h**, **8a–8d**, **5′a–5′h**, **6′a–6′d**) by Fe_3O_4@PFBA–metformin@SO_3H

TABLE 7 Fe_3O_4@PFBA–metformin@SO_3H-catalyzed reaction of 2-piperazinyl quinoxaline or 2-piperazin-1-ylmethyl-1*H*-benzoimidazole with formaldehyde and various substituted isatin derivatives under optimized reaction conditions

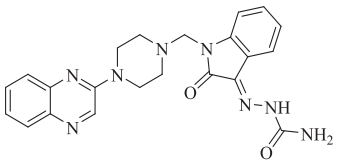	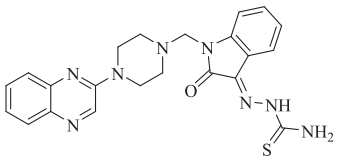	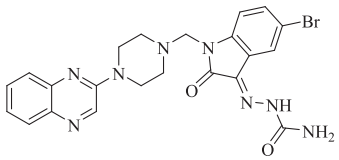
7a Yield (95%) m.p. 186-170 °C	**7b** Yield (95%) m.p. 185 °C	**7c** Yield (98%) m.p. 125-129 °C
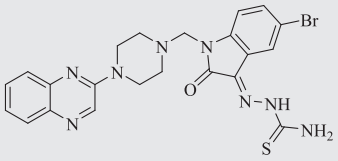	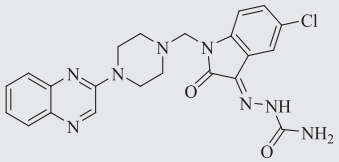	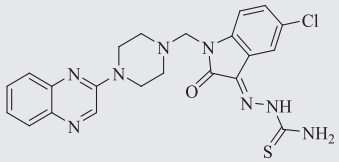
7d Yield (99%) m.p. 132°C–137°C	**7e** Yield (98%) m.p. 177°C	**7f** Yield (99%) m.p. 179°C–183°C
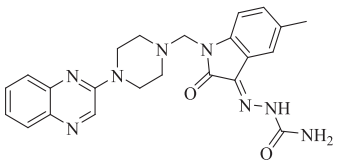	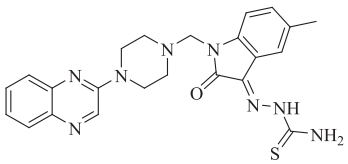	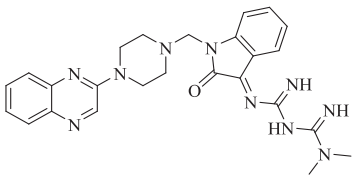
7g Yield (95%) m.p. 192°C	**7h** Yield (97%) m.p. 163°C	**8a** Yield (90%) m.p. 90°C–95°C
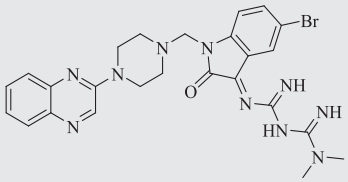	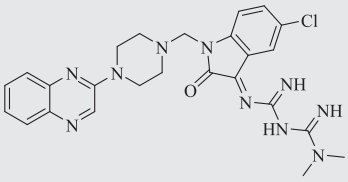	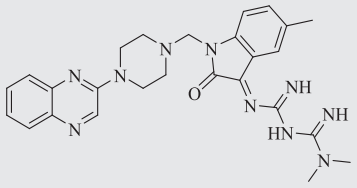
8b Yield (95%) m.p. 108°C	**8c** Yield (95%) m.p. 110°C	**8d** Yield (90%) m.p. 118°C
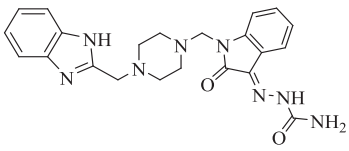	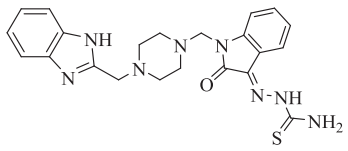	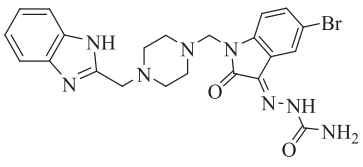

(Continues)

TABLE 7 (Continued)

5′a Yield (90%) m.p. 172°C	**5′b** Yield (95%) m.p. 180°C	**5′c** Yield (95%) m.p. 120°C–123°C
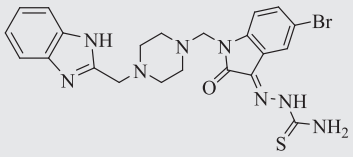	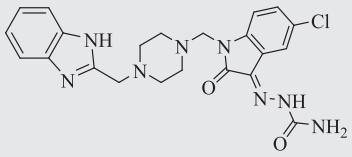	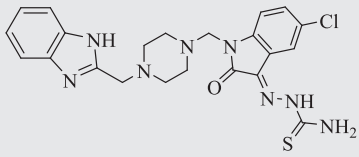
5′d Yield (99%) m.p. 140°C	**5′e** Yield (90%) m.p. 170°C	**5′f** Yield (98%) m.p. 180°C
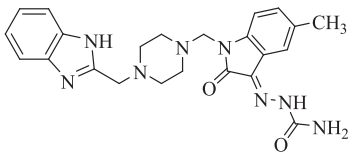	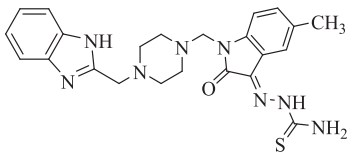	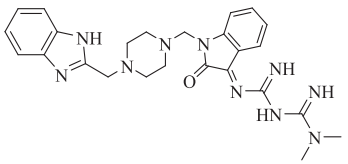
5′g Yield (90%) m.p. 190°C	**5′h** Yield (95%) m.p. 160°C	**6′a** Yield (90%) m.p. 110°C
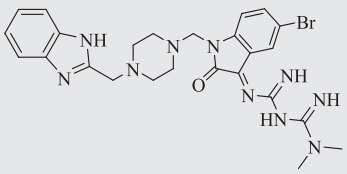	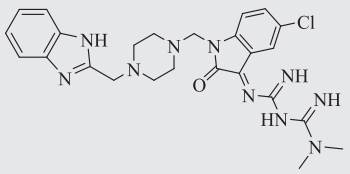	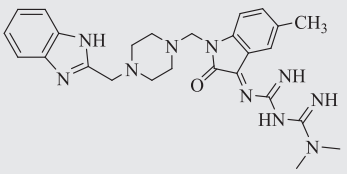
6′b Yield (95%) m.p. 112°C	**6′c** Yield (98%) m.p. 114°C	**6′d** Yield (98%) m.p. 120°C

(Figure 10). The results show good agreement with the fresh catalyst analysis.

3.5 | Hot filtration test

In this experiment, the catalytically active MNPs were removed from the model reaction mixture by a magnet after 50 min, and the filtrate was observed for continual activity. The results display that after eliminating the catalyst, the reaction did not progress, indicating that no catalytically active MNPs in the filtrate. In this case, the hot filtration test can confirm that the reaction proceeds heterogeneously with the stability of the catalyst and no significant leaking of effective SO_3H groups.

3.6 | Calculation of chlorosulfonic acid on the Fe_3O_4@PFBA–metformin@SO_3H

Back titration was used to determine the total percentage of loaded acidic sites onto Fe_3O_4@PFBA–metformin@SO_3H.[31] Certain amount of nanoparticles was first to react with excess KOH standard solution. After 10 min of ultrasonication and completion of the reaction, the nanocatalyst was separated from the reaction mixture using an external magnet. Then, the residual

SCHEME 8 Proposed mechanism for the preparation of Mannich base derivatives of 2-piperazinyl quinoxaline or 2-piperazin-1-ylmethyl-1*H*-benzoimidazole using Fe_3O_4@PFBA–metformin@SO_3H

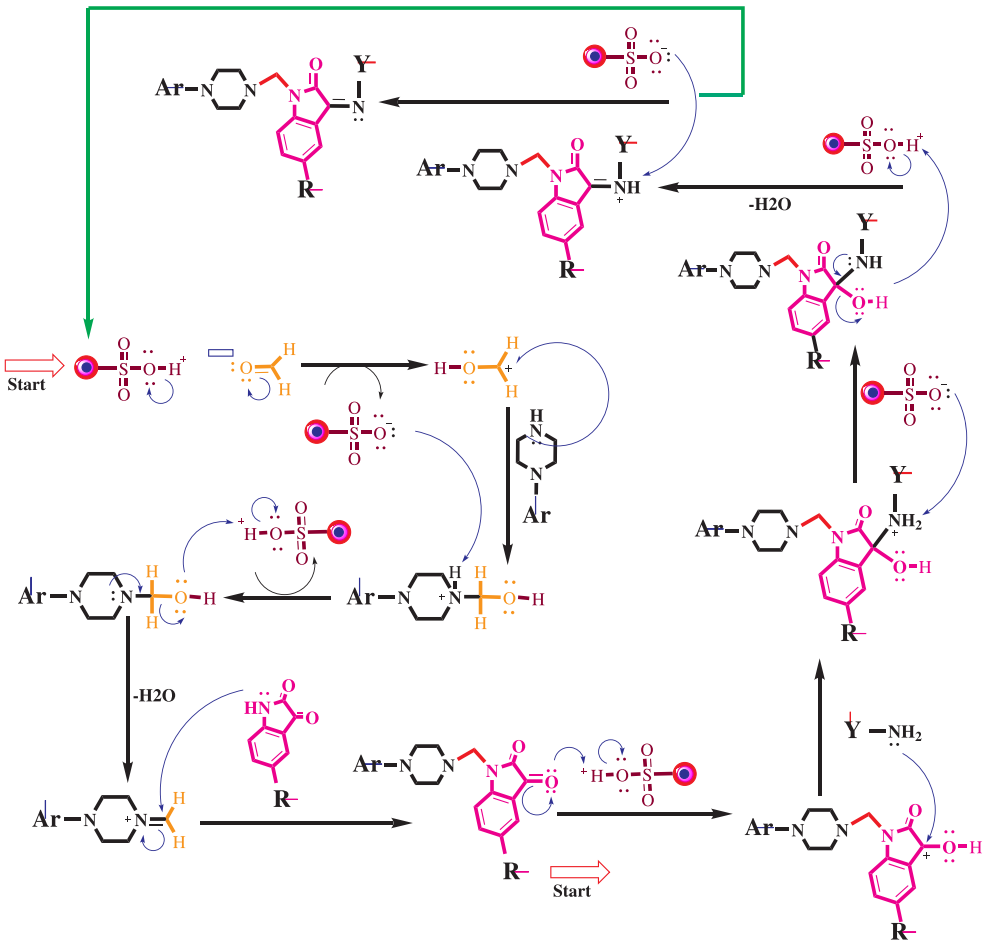

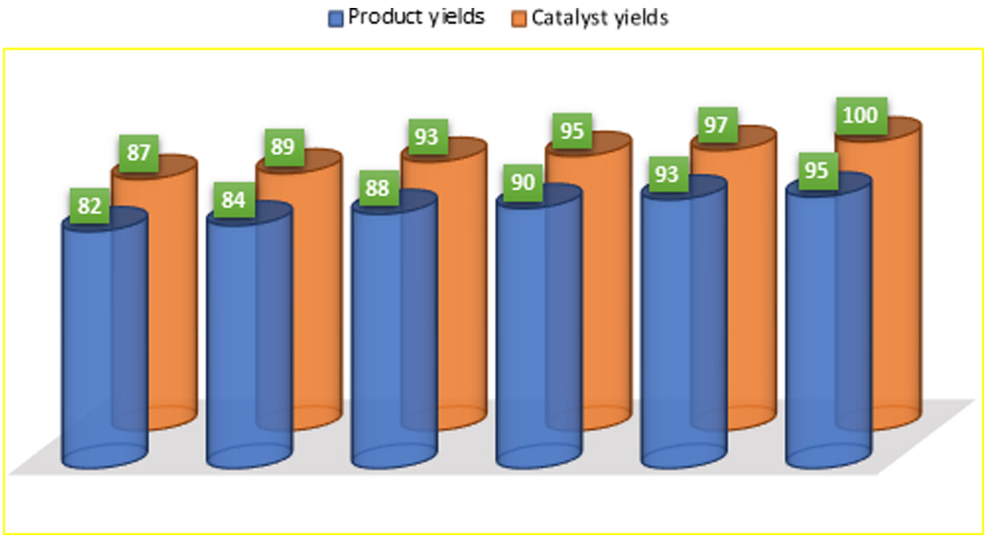

FIGURE 9 Reusability of the nanocatalyst for synthesis of 2-(2-oxoindolin-3-ylidene) hydrazine-1-carboxamide (compound CO_1)

KOH was measured by titration with HCl standard solution in the presence of 0.2-ml indicator phenolphthalein until a faint pink color is obtained. The amount of the acidic groups on individual nanoparticles calculated as 0.93 mmol/g.

3.7 | Calculation of metformin on the Fe_3O_4@PFBA-metformin

After the synthesis of Fe_3O_4@PFBA-metformin, the amount of loaded metformin on Fe_3O_4@PFBA MNPs

TABLE 8 Comparative study the present method with previous works in preparation of quinoxaline-2-ol (compound **II**) and 2-(2-oxoindolin-3-ylidene) hydrazine-1-carboxamide (CO_1)

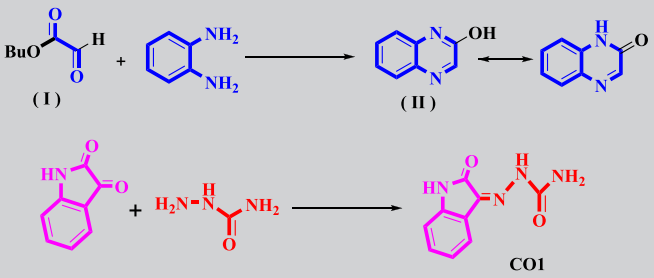

Entry	Catalyst	Solvent	Reaction condition	Time	Yield and product	Reference
1	—	Methanol, toluene	Reflux	2 h	85% compound (**II**)	Fischer et al.[33]
2	Alkaline H_2O_2	Water	Reflux	8 h	86% compound (**II**)	Nasielski and Rypens[34]
3	Selenium (IV) oxide	Water	Reflux	5 h	13% compound (**II**)	Sedov[35]
4	Sodium hydride	Dioxane	R.T	16 h	45% compound (**II**)	Sarges and Lyga[36]
5	Sodium hydroxide	DMF	Heating	8 h	63% compound (**II**)	Hamby and Bauer[37]
6	Nanocatalyst (40 mg)	Ethanol	Reflux	3 h	90% compound (**II**)	This work
7	Pyridine	Methanol	Reflux	300 min	85% compound (CO_1)	Tandon et al.[38]
8	Sodium acetate	Acetic acid	Heating	60 min	88% compound (CO_1)	Somogyi[39]
9	Acetic acid	Ethanol	Reflux	300 min	85% compound (CO_1)	Hall et al.[40]
10	—	Ethanol	Reflux	600 min	90% compound (CO_1)	Atashkar et al.[41]
11	Nanocatalyst (40 mg)	Absolute ethanol	Reflux	150 min	95% compound (CO_1)	This work

was determined by separating the Fe_3O_4@PFBA-metformin MNPs by a simple external magnet; then, the amount of free Metformin in the supernatant was measured by UV spectrophotometer at 233 nm.[32] The total amount of metformin loaded on Fe_3O_4@PFBA was calculated. After completing the whole process and according to the total amount of prepared nanocatalyst at the final step, approximately 0.48 mmol/g of Fe_3O_4@PFBA–metformin@SO_3H is estimated.

$$T0M - TSM = TLM.$$

T0M is the total amount of metformin that entered to the reaction with Fe_3O_4@PFBA, TLM is the total amount of metformin loaded on Fe_3O_4@PFBA-metformin, and TSM is the amount of free metformin in the supernatant.

3.8 | Comparison

To assess the efficiency of this acidic heterogeneous nanocatalyst and methodology, the obtained results from the model reactions were compared with previously reported works, and the results show that Fe_3O_4@PFBA–metformin@SO_3H as an efficient catalyst increases the reaction yields and rate with easy conditions, simple workup, and reduced unwanted by-product (Table 8). As shown in the table, with the cyclocondensation of OPD with butyl 2-oxoacetate (model reaction 1) and the reaction of isatin with semicarbazide (model reaction 4) in the presence of Fe_3O_4@PFBA–metformin@SO_3H as the catalyst, higher yields of products were obtained in shorter reaction time and under milder conditions (Table 3, Entries **2**, **4**, **6**, **1**, **3**, and **5**).

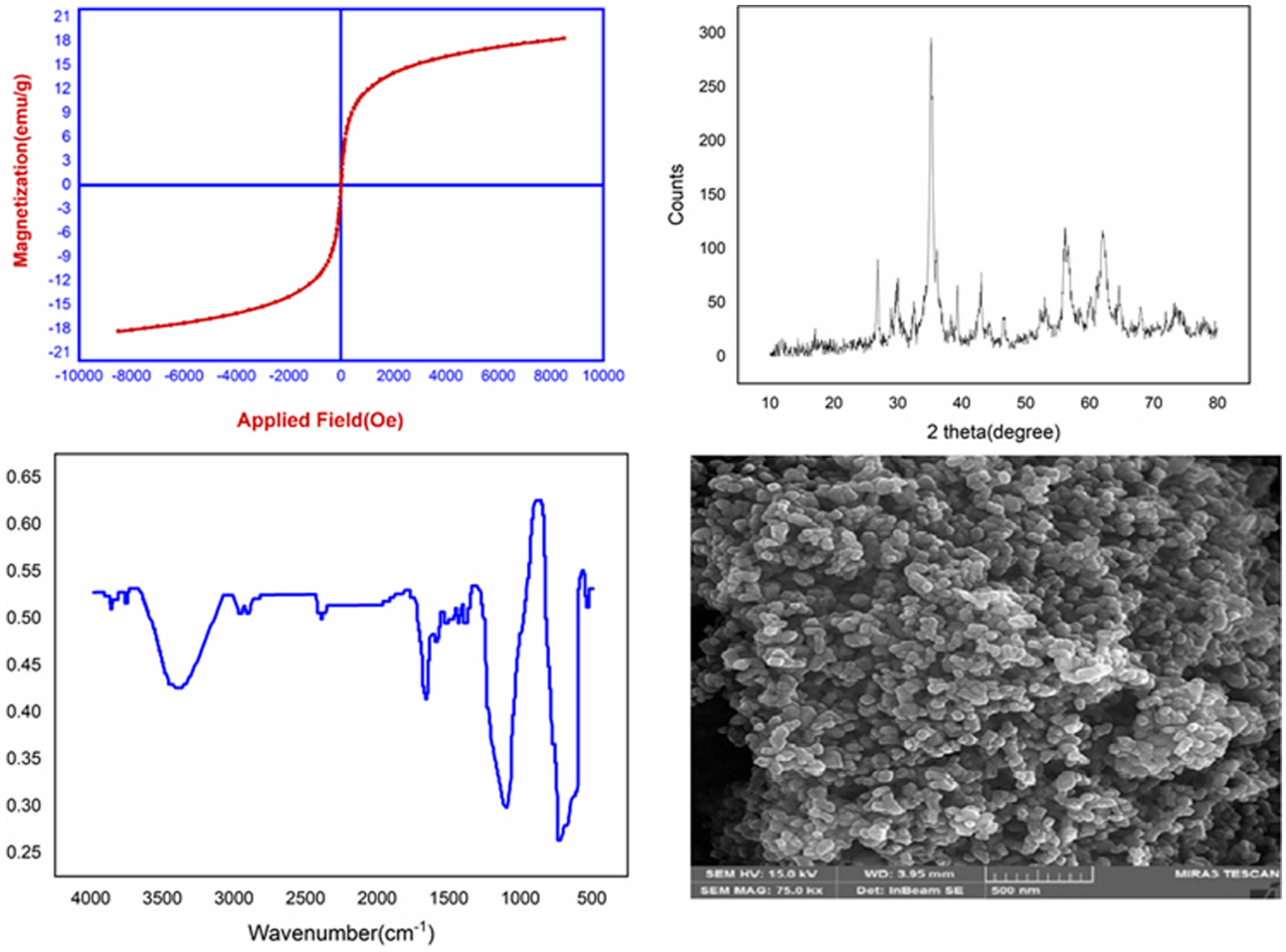

FIGURE 10 Analysis tests of the recovered catalyst

4 | CONCLUSIONS

In summary, in this study, an efficient acidic nanocatalyst (Fe_3O_4@PFBA–metformin@SO_3H) with magnetic properties was developed for one-pot multicomponent cyclocondensation and Mannich reactions, which can reduce the problems of using mineral or homogeneous organic catalysts and traditional methods. A very simple method was used to synthesize the nanocatalysts with core–shell structure; initially, Fe_3O_4 MNPs were synthesized and reported as a core; then, the core was wrapped with a layer of PFBA in the outside, and the PFBA layer was modified by metformin in order to increase the sulfonic groups loading ability. The newly synthesized nanocatalyst was characterized structurally by SEM, EDX, XRD, and VSM spectroscopy. According to the successful catalytic performance of Fe3O4@PFBA–metformin@SO3H in the current study, we aspire that this novel acidic nanocatalyst can have extensive applications in different kinds of acid-based catalytic reactions. Fe3O4@PFBA–metformin@SO3H is a green, eco-friendly, nontoxic, economic, and easy workup nanocatalyst with magnetic properties, which the latter guarantees its easy recovery by a simple magnet. This newly synthesized magnetic nanocatalyst can be reused several times with no remarkable drop in the catalytic activity.

FUNDING INFORMATION

The main part of this work was connected to the PhD thesis of Dr. Zohreh Esam from the Faculty of Pharmacy, Mazandaran University of Medical Sciences.

AUTHOR CONTRIBUTIONS

Zohreh Esam: Data curation; formal analysis; funding acquisition; project administration; resources; software. **Malihe Akhavan:** Investigation; methodology.

DATA AVAILABILITY STATEMENT

The data that support the findings of this study are available on request from the corresponding author. The data are not publicly available because of privacy/ethical restrictions.

ORCID

Zohreh Esam https://orcid.org/0000-0003-3126-9507
Malihe Akhavan https://orcid.org/0000-0001-6041-6989
Ahmadreza Bekhradnia https://orcid.org/0000-0002-7155-4532

REFERENCES

[1] M. Tajbakhsh, G. B. Chalmardi, A. Bekhradnia, R. Hosseinzadeh, N. Hasani, M. A. Amiri, *Spectrochim. Acta a* **2018**, *189*, 22.
[2] A. Shafiee, M. Z. Kassaee, A. R. Bekhradnia, *J. Heterocyclic Chem.* **2007**, *44*, 471.
[3] M. Baumann, I. R. Baxendale, *Beilstein J. Org. Chem.* **2013**, *9*, 2265.
[4] S. A. Shintre, D. Ramjugernath, M. S. Islam, R. Mopuri, C. Mocktar, N. A. Koorbanally, *Med. Chem. Res.* **2017**, *26*, 2141.
[5] Z. Ghanbarimasir, A. Bekhradnia, K. Morteza-Semnani, A. Rafiei, N. Razzaghi-Asl, M. Kardan, *Spectrochim. Acta a* **2018**, *194*, 21.
[6] Ü. Yılmaz, H. Küçükbay, N. Şireci, M. Akkurt, S. Günal, R. Durmaz, M. Nawaz Tahir, *Appl. Organomet. Chem.* **2011**, *25*, 366.
[7] F. Rajabi, D. Alves, R. Luque, *Molecules* **2015**, *20*, 20709.
[8] R. Teimuri-Mofrad, S. Tahmasebi, E. Payami, *Appl. Organomet. Chem.* **2019**, *33*, e4773.
[9] D. M. Ruiz, J. C. Autino, N. Quaranta, P. G. Vázquez, G. P. Romanelli, *Sci. World J.* **2012**, *2012*, 1.
[10] A. Fallah, M. Tajbakhsh, H. Vahedi, A. Bekhradnia, *Res CHEM INTERMEDIAT* **2017**, *43*, 29.
[11] M. Akhavan, N. Foroughifar, H. Pasdar, A. Khajeh-Amiri, A. Bekhradnia, *Transition Met. Chem.* **2017**, *42*, 543.
[12] M. Arghan, N. Koukabi, E. Kolvari, *Appl. Organomet. Chem.* **2019**, *33*, e4823.
[13] Z. Abbasi, S. Rezayati, M. Bagheri, R. Hajinasiri, *Chin. Chem. Lett.* **2017**, *28*, 75.
[14] S. Sajjadifar, S. Rezayati, A. Shahriari, S. Abbaspour, *Appl. Organomet. Chem.* **2018**, *32*, e4172.
[15] SN. Vajekar, GS. Shankarling, Z. Arzehgar, S. Abbaspour, M. Torabi Jafroudi, *ChemistrySelect*. **2018**, *3*(21), 5848.
[16] S. Mohammad Vahdat, S. Baghery, *Comb. Chem. High Throughput Screening* **2013**, *16*, 618.
[17] G. Brahmachari, S. Laskar, P. Barik, *RSC Adv.* **2013**, *3*, 14245.
[18] K. B. Harsha, S. Rangappa, H. D. Preetham, T. R. Swaroop, M. Gilandoust, K. S. Rakesh, K. S. Rangappa, *ChemistrySelect* **2018**, *3*, 5228.
[19] K. Dânoun, Y. Essamlali, O. Amadine, H. Mahi, M. Zahouily, *BMC CHEM.* **2020**, *14*, 1.
[20] M. Shamsi-Sani, F. Shirini, M. Abedini, M. Seddighi, *Res. Chem. Intermed.* **2016**, *42*, 1091.
[21] A. Shaabani, Z. Hezarkhani, *Appl. Organomet. Chem.* **2017**, *31*, e3542.
[22] M. Kalhor, Z. Zarnegar, Z. Seyedzade, S. Banibairami, *Curr. Org. Synth.* **2020**, *17*, 117.
[23] F.-C. Zheng, Q.-W. Chen, L. Hu, N. Yan, X.-K. Kong, *Dalton Trans.* **2014**, *43*, 1220.
[24] R. Ghorbani-Vaghei, V. Izadkhah, *Appl. Organomet. Chem.* **2018**, *32*, e4025.
[25] M. Kidwai, A. Jain, R. Poddar, S. Bhardwaj, *Appl. Organomet. Chem.* **2011**, *25*, 335.
[26] Z. Esam, M. Akhavan, A. Bekhradnia, M. Mohammadi, S. Tourani, *Catal. Lett.* **2020**, *8*, 20.
[27] W. C. Lumma Jr., R. D. Hartman, W. S. Saari, E. L. Engelhardt, V. J. Lotti, C. A. Stone, *J. Med. Chem.* **1981**, *24*, 93.
[28] H. Bektaş, B. B. Sökmen, S. Aydın, E. Menteşe, A. Bektaş, G. Dilekçi, *J. Heterocycl. Chem.* **2020**, *57*(5), 2234.
[29] G. Ashit, G. William, W. F. Wasley Jan, 1-(2-Naphthyl) and 1-(2-azanaphthyl)-4-(1-phenylmethyl)piperazines being dopamine d 4? Receptor subtype ligands. European Patent Office Publ. of Application with search report EP19980952391. 20 Oct **1998**.
[30] H. Veisi, S. Taheri, S. Hemmati, *Green Chem.* **2016**, *18*, 6337.
[31] C. Y. Wen, J. Y. Sun, *ChemistrySelect* **2017**, *33*, 10885.
[32] S. K. Chinnaiyan, D. Karthikeyan, V. R. Gadela, *Pharmaceutical Nanotechnology.* **2018**, *4*, 253.
[33] G. M. Fischer, M. Isomäki-Krondahl, I. Göttker-Schnetmann, E. Daltrozzo, A. Zumbusch, *Chem. - a Eur. J.* **2009**, *15*, 4857.
[34] J. Nasielski, C. Rypens, *J. Phys. Org. Chem.* **1994**, *7*, 545.
[35] Y. A. Sedov, *Chem. Heterocycl. Compd.* **1983**, *19*, 217.
[36] R. Sarges, J. W. Lyga, *J. Heterocyclic Chem.* **1988**, *25*, 1475.
[37] J. M. Hamby, L. Bauer, *J. Heterocyclic Chem.* **1987**, *24*, 1013.
[38] S. S. Tandon, S. D. Bunge, J. Sanchiz, L. K. Thompson, *Inorg. Chem.* **2012**, *51*, 3270.
[39] L. Somogyi, *Bull. Chem. Soc. Jpn.* **2001**, *74*, 873.
[40] M. D. Hall, N. K. Salam, J. L. Hellawell, H. M. Fales, C. B. Kensler, J. A. Ludwig, G. Szakács, D. E. Hibbs, M. M. Gottesman, *J. Med. Chem.* **2009**, *52*, 3191.
[41] S. Shylesh, V. Schünemann, W. R. Thiel, *Angew. Chem. Int. Ed.* **2010**, *49*(20), 3428.

SUPPORTING INFORMATION

Additional supporting information may be found online in the Supporting Information section at the end of this article.

How to cite this article: Esam Z, Akhavan M, Bekhradnia A. One-pot multicomponent synthesis of novel 2-(piperazin-1-yl) quinoxaline and benzimidazole derivatives, using a novel sulfamic acid functionalized Fe_3O_4 MNPs as highly effective nanocatalyst. *Appl Organomet Chem*. 2020;e6005. https://doi.org/10.1002/aoc.6005